

The runaway growth of intermediate-mass black holes in dense star clusters

Simon F. Portegies Zwart^{1,2}

and

Stephen L. W. McMillan³

¹ Astronomical Institute “Anton Pannekoek”, University of Amsterdam, Kruislaan 403, 1098 SH Amsterdam, NL; spz@science.uva.nl

² Section Computational Science, University of Amsterdam, Kruislaan 403, 1098 SH Amsterdam, NL

³ Dept. of Physics, Drexel University, Philadelphia, PA 19104, USA; steve@kepler.physics.drexel.edu

Subject headings: stellar dynamics – binaries (including multiple): close – globular clusters: general – Galaxies: bulges – galaxies: star clusters – methods: N-body simulations

ABSTRACT

We study the growth rate of stars via stellar collisions in dense star clusters, calibrating our analytic calculations with direct N -body simulations of up to 65536 stars, performed on the GRAPE family of special-purpose computers. We find that star clusters with initial half-mass relaxation times $\lesssim 25$ Myr are dominated by stellar collisions, the first collisions occurring at or near the point of core collapse, which is driven by the segregation of the most massive stars to the cluster center, where they end up in hard binaries. The majority of collisions occur with the same star, resulting in the runaway growth of a supermassive object. This object can grow up to $\sim 0.1\%$ of the mass of the entire star cluster and could manifest itself as an intermediate-mass black hole (IMBH). The phase of runaway growth lasts until mass loss by stellar evolution arrests core collapse. Star clusters older than about 5 Myr and with present-day half-mass relaxation times $\lesssim 100$ Myr are expected to contain an IMBH.

1. Introduction

Using the *Chandra* X-ray observatory, Kaaret et al. (2000; 2001) and Matsumoto et al. (2000; 2001) recently discovered nine bright X-ray sources in the irregular galaxy M82. Their brightest source (No. 7 in Table 1 of Matsumoto et al. 2001) has a luminosity of $9 \times 10^{40} \text{ergs}^{-1}$ in the 0.2–10 KeV band, corresponding to the Eddington luminosity of a $\sim 600 M_{\odot}$ compact object. The high luminosity and rather soft X-ray spectrum of the object indicates that it may be an intermediate-mass black hole (IMBH) with a mass of at least $600 M_{\odot}$ (Kaaret et al. 2001; Matsumoto et al. 2001).

An optical follow-up in the infrared (J, H, and K' -bands) with the CISCO instrument on the SUBARU telescope revealed a star cluster with an estimated mass of a few $10^6 M_{\odot}$ at a position consistent with the X-ray location of the IMBH (Harashima et al. 2001). This star cluster appears to be very young ($\lesssim 10$ Myr), as it is extremely blue and expanding shells of molecular gas have been discovered in its vicinity (Matsushita et al. 2000), typical for a star-forming region of a few million years.

Matsushita et al. (2000) estimate that the environment has an age of only a few million years.

More unusually bright X-ray point sources have been discovered in the early spiral galaxies NGC 2403 (Kotoku et al. 2000) and NGC 4565 (Mizuno, et al. 1999). Most remarkable, however, is the discovery of many bright X-ray sources in the “Antennae” system (NGC 4038/4039) by Fabbiano et al. (2001), Zazas & Fabbiano (2002) and Zazas et al. (2002), also using *Chandra*. These authors conclude that many of these sources may be $\gtrsim 100 M_{\odot}$ accreting black holes (although alternative explanations exist—see e.g. Mizuno 1999; King et al. 2001). The Antennae contain many young star clusters with characteristics similar to those found in M82 (Mengel et al. 2001). However, it is not yet clear how many of the X-ray sources in the Antennae are associated with these clusters (Zazas & Fabbiano 2002). There may also be an example of an IMBH in our own Galaxy, as recent reverberation mapping of the globular cluster M15 by Gebhardt et al. (2000, 2001, and private communication) strongly suggests that the cluster may harbor a $\sim 2500 M_{\odot}$ black hole at its center.

Several possible mechanisms for forming IMBHs in star clusters have recently been suggested. Miller & Hamilton (2001) have studied the possibility that an IMBH may form slowly (on a Hubble time scale) by occasionally encountering and devouring other cluster stars. Mouri & Taniguchi (2002) have proposed a much more rapid black-hole merger mechanism, operating in very high-density (10^6 black holes pc^{-3}) environments on time scales as short as $\sim 10^7$ yr. In this paper we consider the possibility of forming a massive object in a young star cluster due to repeated collisions during an early phase of core collapse.

Sanders (1970), Lee (1987), and Quinlan & Shapiro (1990) have studied the possibility of collision runaways in spherical stellar systems of $\gtrsim 10^7$ stars with high ($> 100 \text{km s}^{-1}$) velocity dispersions. All studies began with stars of equal masses and found that, for sufficiently high densities and velocity dispersions, runaway mergers could indeed occur. Quinlan & Shapiro observed that the collision time scale for massive stars decreases faster with increasing mass than does the main-sequence lifetime, and concluded that clusters with initial relaxation times of $1\text{--}5 \times 10^8$ years could grow a massive $\gtrsim 100 M_{\odot}$ object by multiple mergers. Sanders’ (1970) Monte-Carlo calculations neglected the effects of mass segregation and found collision runaways only after mergers had driven the cluster into a state of high central density. However, in the self-consistent Fokker–Planck models of Lee and Quinlan & Shapiro, the runaway started well before core collapse occurred. All authors concluded that runaways would not occur in clusters containing less than $\sim 10^6 - 10^7$ stars because three-body binary heating in small N -systems provided sufficient energy to reverse core collapse before the runaway process could begin.

In contrast to the studies just described, the models discussed in this paper begin with a broad range of stellar masses. Vishniac (1978) demonstrated that a Salpeter (1955) initial mass function is Spitzer (1969) unstable. As a result, young star clusters may experience core collapse on the time scale on which the most massive stars segregate to the cluster center. This time scale may be much shorter than the main sequence lifetimes of the stars involved. Vishniac suggested that such a prompt collapse might lead to the formation of a massive compact object. We find that early core collapse in a relatively low- N star cluster may result in a collision runaway, so long as the most massive stars remain on the main sequence while the collapse occurs.

The possibility of multiple collisions involving the same star in a dense star cluster was demonstrated convincingly by Portegies Zwart et al. (1999), using the special-purpose GRAPE-4 (Makino et al. 1997) to speed up their direct N -body calculations with up to 12288 stars. They concluded that, even in small clusters, runaway collisions may lead to the growth of a single massive star. The earlier arguments that three-body binary heating would drive the expansion of the cluster core appear to be unimportant in these

simulations, as mergers between stars tend to destroy binaries before they can heat the cluster effectively. Indeed, in contrast to the underlying assumptions of previous collision studies, dynamically formed binaries in dense clusters act as a *catalyst* for stellar mergers, boosting the collision rate far beyond the simple two-body expressions used in earlier work. The N-body simulations covered a rather limited part of the available parameter space, but the initial conditions were selected to mimic known dense star clusters in the Galaxy and the Large Magellanic Cloud.

If the bright X-ray source in M82 does indeed correspond to a compact object of $\gtrsim 600 M_\odot$, this IMBH could have been formed by a collision runaway resulting from collapse of the cluster core early in the cluster. In fact, as we will see, it is quite natural to expect a $\sim 10^3 M_\odot$ black hole in a million-solar-mass star cluster. We begin by deriving (§2) some simple analytic expressions describing the dynamical behavior observed in cluster simulations. In §3 we calibrate these relations using direct N -body simulations. We then (§4) extend these results to derive simple relations between black-hole formation and cluster parameters.

2. Runaway growth of a massive object in a dense star cluster

2.1. Core collapse and the first collision

A star cluster is a self-gravitating group of stars. So long as stellar evolution remains relatively unimportant, the cluster’s dynamical evolution is dominated by two-body relaxation, with characteristic time scale (Spitzer, 1987)

$$t_{\text{rlx}} = \left(\frac{R_c^3}{GM_c} \right)^{1/2} \frac{N_c}{8 \ln \Lambda_c}, \quad (1)$$

the half-mass relaxation time. Here G is the gravitational constant, M_c is the total mass of the cluster, $N_c \equiv M_c/\langle m \rangle$ is the number of stars and R_c is the characteristic (half-mass) radius of the cluster. The Coulomb logarithm $\ln \Lambda_c \simeq \ln(0.1N_c) \sim 10$ typically. In convenient units the two-body relaxation time becomes

$$t_{\text{rlx}} \simeq 1.9 \text{ Myr} \left(\frac{R_c}{1 \text{ pc}} \right)^{3/2} \left(\frac{M_c}{1 M_\odot} \right)^{1/2} \left(\frac{1 M_\odot}{\langle m \rangle} \right) (\ln \Lambda_c)^{-1}. \quad (2)$$

The dynamical evolution of the star cluster drives it toward core collapse (Antonov 1962; Spitzer & Hart, 1971) in which the central density runs away to a formally infinite value in a finite time. In an isolated cluster in which all stars have the same mass, core collapse occurs in a time $t_{\text{cc}} \simeq 15 t_{\text{rlx}}$ (Cohn 1980).

Realistic clusters have a broad range in initial stellar masses, generally from $m_{\text{min}} \simeq 0.1 M_\odot$ to $m_{\text{max}} \simeq 100 M_\odot$, with mean mass $\langle m \rangle$ ranging from $\sim 0.39 M_\odot$ (Salpeter 1955) to about $0.65 M_\odot$ (Scalo 1986), depending on the specific mass function adopted. During the early evolution of the cluster, massive stars sink toward the cluster center via dynamical friction. Approximating the cluster structure as an isothermal sphere, we find (Binney & Tremaine 1987, Eq. 7-25) that a star of mass m at distance r from the cluster center drifts inward at a rate given by

$$r \frac{dr}{dt} = -0.43 \frac{Gm}{V_c} \ln \Lambda_c, \quad (3)$$

Here V_c is the cluster velocity dispersion. Using Eq. 2, we can integrate Eq. 3 with respect to time to obtain the dynamical friction inspiral time scale

$$t_{\text{f}} = 3.3 \frac{\langle m \rangle}{m} t_{\text{rlx}}. \quad (4)$$

This is the time taken for a star of mass m to sink to the cluster center from a circular orbit at initial distance $r \gg r_{\text{core}}$.

In a multi-mass system, core collapse is driven by the accumulation of the most massive stars in the cluster center. This process takes place on a dynamical friction time scale (Eq. 4). Empirically, we find, for initial mass functions of interest here, that core collapse (actually, the appearance of the first persistent dynamically formed binary systems) occurs at about

$$t_{\text{cc}} \simeq 0.20 t_{\text{rlx}}. \quad (5)$$

This core collapse time is taken in the limit where stellar evolution is unimportant, i.e. where stellar mass loss is negligible and the most massive stars survive until they reach the cluster center.

The collapse of the cluster core may initiate physical collisions between stars. The product of the first collision is likely to be among the most massive stars in the system, and to be in the core. This star is therefore likely to experience subsequent collisions, resulting in a collision runaway (see Portegies Zwart et al. 1999). The maximum mass that can be grown in a dense star cluster if all collisions involve the same star is m_{r} , where

$$\frac{dm_{\text{r}}}{dt} = \mathcal{N}_{\text{coll}} \langle \delta m \rangle_{\text{coll}}. \quad (6)$$

Here $\mathcal{N}_{\text{coll}}$ and $\langle \delta m \rangle_{\text{coll}}$ are the average collision rate and the average mass increase per collision (assumed independent). We now discuss these quantities in more detail. In §3 we present some N-body results that both motivated and calibrate the following discussion.

2.2. The collision rate $\mathcal{N}_{\text{coll}}$

A key result from our simulations is the fact that collisions between stars generally occur in dynamically formed (“three-body”) binaries. The collision rate is therefore closely related to the binary formation rate, which we now estimate.

The flux of energy through the half-mass radius of a cluster during one half-mass relaxation time is on the order of 10% of the cluster potential energy, largely independent of the total number of stars or the details of the cluster’s internal structure (Goodman 1987). For a system without primordial binaries this flux is produced by heating due to dynamically formed binaries (Makino & Hut 1990). It is released partly in the form of scattering products which remain bound to the system, and partly in the form of potential energy removed from the system by escapers recoiling out of the cluster (Hut & Inagaki 1985). Makino & Hut argue, for an equal-mass system, that a binary generates an amount of energy on the order of $10^2 kT$ via binary–single-star scattering (where the total kinetic energy of the stellar system is $\frac{3}{2} N_c kT$). This quantity originates from the minimum binding energy of a binary that can eject itself following a strong encounter. Assuming that the large-scale energy flux in the cluster is ultimately powered by binary heating in the core. It follows that the required formation rate of binaries via three-body encounters is

$$n_{\text{bf}} \simeq 10^{-3} \frac{N_c}{t_{\text{rlx}}}. \quad (7)$$

For systems containing significant numbers of primordial binaries, which segregate to the cluster core, equivalent energetic arguments (Goodman & Hut 1989) lead to a similar scaling for the net rate at which binary encounters occur in the core.

The above arguments apply to star clusters comprising identical point-mass stars. In a cluster with a range of stellar masses, three-body binaries generally form from stars which are more massive than average. After repeated exchange interactions, the binary will consist of two of the most massive stars in the cluster. Conservation of linear momentum during encounters with lower mass stars means that the binary receives a smaller recoil velocity, making it less likely to be ejected from the cluster. The binary must therefore be considerably harder— $\gtrsim 10^3 kT$ —before it is ejected following an encounter with another star (see Portegies Zwart & McMillan 2000).

However, taking the finite sizes of real stars into account, it is quite likely that such a hard binary experiences a collision rather than being ejected. A strong encounter between a single star and a hard binary generally results in a resonant interaction. Three stars remain in resonance until at least one of them escapes, or a collision reduces the three-body system to a stable binary. For harder binaries it becomes increasingly likely that a collision occurs instead of ejection (McMillan 1986). In the calculations of Portegies Zwart et al. (1999) most binaries experience a collision at a binding energy of order $10^2 kT$, considerably smaller than the binding energy required for ejection. Accordingly, we retain the above estimate of the binary formation rate (Eq. 7) and conclude that the collision rate per half-mass relaxation time is

$$\mathcal{N}_{\text{coll}} \sim 10^{-3} f_c \frac{N_c}{t_{\text{rlx}}}. \quad (8)$$

Here we introduce $f_c \leq 1$, the effective fraction of dynamically formed binaries that produce a collision. Note again that Eq. 8 is valid only in the limit where stellar evolution is unimportant.

The most massive star in the cluster is typically a member of the interacting binary and therefore dominates the collision rate. Subsequent collisions cause the runaway to grow in mass, making it progressively less likely to escape from the cluster. The star which experiences the first collision is therefore likely to participate in subsequent collisions. The majority of collisions thus involve one particular object—the runaway merger—generally selected by its high initial mass and proximity to the cluster center (see Portegies Zwart et al. 1999).

For systems containing many primordial binaries the above argument must be modified. Since dynamically formed binaries tend to be fairly soft—a few kT —we expect that the fraction of interactions with primordial binaries leading to collision is comparable to the value f_c above. However, a critical difference is that, in systems containing many binaries, the collisions involve many different pairs of stars, not just the binary containing the massive runaway. For our proposed runaway scenario to operate, we must assume that high-mass binaries are rapidly destroyed or merge following interactions in the core, in which case the above arguments apply. We note that, once a runaway begins, binaries have large interaction cross sections and hence are likely to participate in the runaway process. From the point of view of producing massive merger products, the worst-case scenario would be a substantial primordial population of wide high-mass binaries. We are currently carrying out N-body simulations to investigate the behavior of such systems.

2.3. Average mass increase per collision

Once begun, the collision runaway dominates the collision cross section. The average mass increase per collision depends on the characteristics of the mass function in the cluster core. A lower limit for stars which participate in collisions can be derived from the degree of segregation in the cluster. Inverting Eq. 4 results in an estimate (still assuming an isothermal sphere) of the minimum mass of a star that can reach

the cluster core in time t due to dynamical friction:

$$m_f = 1.9M_\odot \left(\frac{1 \text{ Myr}}{t} \right) \left(\frac{R_c}{1 \text{ pc}} \right)^{3/2} \left(\frac{M_c}{1 M_\odot} \right)^{1/2} (\ln \Lambda_c)^{-1}. \quad (9)$$

Thus, at time t and for a given mass m , there is a maximum radius $r(t)$ inside of which stars of mass m will have segregated to the core. The stars contributing to the growth of the runaway are likely to be among those more massive than m_f , because their number density in the core is enhanced by mass segregation, their collision cross sections are larger, and they contribute more to $\langle \delta m \rangle_{\text{coll}}$ when they do collide.

The shape of the central mass function of a segregated cluster is not trivial to derive. In thermal equilibrium, the central number densities of stars of different masses would be expected to scale as

$$n_0(m) \sim m^{3/2} \frac{dN}{dm}, \quad (10)$$

where dN/dm is the global (Scalo) initial mass function, which scales roughly as $m^{-2.7}$ at the high-mass end ($m \gtrsim 10M_\odot$). However, as discussed in §3, the distribution of secondary masses (i.e. the masses of the lighter stars participating in collisions) does not follow the above simple relation. Rather, we find that stars in the core do not reach thermal equilibrium (a result generally consistent with earlier findings by Chernoff and Weinberg 1990 and Joshi, Nave & Rasio 2001), and that the dynamical nature of the collisional processes involved mean that more massive stars tend to be consumed before lower-mass stars arrive in the core. In addition, most collisions involve three-body binary formation and binary interactions in a multi-mass environment, further complicating the connection between stellar densities and secondary masses.

Empirically, we find that the secondary mass distribution is quite well fit by a power-law, $dN/dm \propto m^{-2.3}$ (coincidentally very close to a Salpeter distribution). Integrating this expression from a minimum mass of m_f (and ignoring the upper limit) results in a mean mass increase per collision of

$$\langle \delta m \rangle_{\text{coll}} \simeq 4m_f. \quad (11)$$

We neglect stars with masses less than m_f . Substitution of Eq. 1 into Eq. 9 and Eq. 11 then results in a mass increase per collision of

$$\langle \delta m \rangle_{\text{coll}} \simeq 4 \frac{t_{\text{rlx}}}{t} \langle m \rangle \ln \Lambda_c. \quad (12)$$

Taken over the entire “collisional” lifetime of the core, it is perhaps not surprising that the net distribution of secondary masses tends to follow the overall distribution of high-mass stars.

2.4. Lifetime of a cluster in a static tidal field

With simple expressions for $\mathcal{N}_{\text{coll}}$ and $\langle \delta m \rangle_{\text{coll}}$ now in hand, we return to the determination of the runaway growth rate (Eq. 6). The evaporation of a star cluster which fills its Jacobi surface in an external potential is driven by tidal stripping. Portegies Zwart et al (2001a) have studied the evolution of young compact star clusters within ~ 200 pc of the Galactic center. Their calculations employed direct N -body integration, including the effects of both stellar and binary evolution and the (static) external influence of the Galaxy, and made extensive use of the GRAPE-4 (Makino et al. 1997) special-purpose computer. They found that the mass of a typical model cluster decreased almost linearly with time:

$$M_c = M_{c0} \left(1 - \frac{t}{t_{\text{disr}}} \right). \quad (13)$$

Here M_{c0} is the mass of the cluster at birth and t_{disr} is the cluster’s disruption time. Portegies Zwart et al. (2001a) found that their model clusters dissolved within about 30% of the two-body relaxation time at the tidal radius (defined by substituting the tidal radius instead of the virial radius in Eq. 1). In terms of the half-mass relaxation time, we find $t_{\text{disr}} = 1.6\text{--}5.4 t_{\text{rlx}}$, depending on the initial density profile (the range corresponds to King [1966] dimensionless depths $W_0 = 3\text{--}7$; more centrally condensed clusters live longer).

Substituting Eqs. 8 and 12 into Eq. 6, and defining $M_{c0} = N_c \langle m \rangle$ to rewrite Eq. 13 in terms of the number of stars in the cluster, we find

$$\begin{aligned} \frac{dm_r}{dt} &= 4 \times 10^{-3} f_c \frac{N_c \langle m \rangle \ln \Lambda_c}{t} \\ &= 4 \times 10^{-3} f_c M_{c0} \ln \Lambda_c \left(\frac{1}{t} - \frac{1}{t_{\text{disr}}} \right). \end{aligned} \quad (14)$$

Integrating from $t = t_{\text{cc}}$ to $t = t_{\text{disr}}$ results in

$$m_r = m_{\text{seed}} + 4 \times 10^{-3} f_c M_{c0} \ln \Lambda_c \left[\ln \left(\frac{t_{\text{disr}}}{t_{\text{cc}}} \right) + \frac{t_{\text{cc}}}{t_{\text{disr}}} - 1 \right]. \quad (15)$$

Here m_{seed} is the seed mass of the star which initiates the runaway growth, most likely one of the most massive stars initially in the cluster. With $t_{\text{cc}} \simeq 0.2 t_{\text{rlx}}$, Eq 15 reduces to

$$m_r = m_{\text{seed}} + 4 \times 10^{-3} f_c M_{c0} \gamma \ln \Lambda_c, \quad (16)$$

where $\gamma \simeq \ln t_{\text{disr}}/t_{\text{cc}} + t_{\text{cc}}/t_{\text{disr}} - 1 \sim 1$.

3. Results of N -body simulations

The development of the GRAPE family of special-purpose computers makes it relatively straightforward to test and tune the above simple model using direct N -body calculations. Tab. 1 summarizes the results of an extensive series of detailed N -body simulations of core collapse and stellar collisions in dense star clusters containing up to 65536 stars. These simulations were performed using the “Starlab” software environment (see Portegies Zwart et al. 2001b) running on the GRAPE-6 (Makino 2000). The calculations were performed with initially single stars but, as just discussed, the presence of primordial binaries is not likely to change the picture qualitatively. To expand on these findings, we have performed an additional series of simulations with $\sim 10^4$ stars using the same software and hardware. Further simulations of systems containing substantial numbers of primordial binaries are in progress, but are much more time consuming, due to the complexity of following binary and multiple encounters in a large- N context.

3.1. Core collapse

In our isolated star clusters (three calculations) with 10^4 identical single point masses distributed as a Plummer model, core collapse occurs at $t_{\text{cc}} \simeq 15.2 \pm 0.1 t_{\text{rlx}}$. This result is consistent with earlier calculations of e.g., Cohn (1980) and Makino (1996). Doubling the mass of 20% of the stars reduced the core collapse time to $t_{\text{cc}} \simeq 7.2 t_{\text{rlx}}$. Making 20% of the stars 10 or 100 times more massive reduced the time of core collapse further, to $t_{\text{cc}} \simeq 1.4 t_{\text{rlx}}$ and $t_{\text{cc}} \simeq 0.16 t_{\text{rlx}}$, respectively.

The more realistic models of Portegies Zwart et al. (1999) with 6144 and 12288 single stars drawn from a Scalo (1986) initial mass function also include mass loss from stellar evolution. The initial density

distributions for these models were $W_0 = 6$ King (1966) models. Core collapse in these models occurred at $t_{\text{cc}} \simeq 0.19 \pm 0.08 t_{\text{rlx}}$. The slightly later collapse compared to the models just described, containing 10^4 identical point masses and a heavy component, may be attributable to the rather different mass function, as well as to stellar mass loss, which tends to delay core collapse.

3.2. Collision rate

Relaxing the assumption of point masses to include finite stellar sizes introduces collisions into our models. In all calculations, the first collision occurred shortly after the formation of the first $\gtrsim 10 kT$ binary by a three-body encounter, i.e. close to the time of core collapse. When stars were given unrealistically large radii (100 times larger than normal), the first collisions occurred only slightly (about 5%) earlier.

As discussed earlier, the first star to experience a collision was generally one of the most massive stars in the cluster; this star then became the target for further collisions. In models with initial relaxation times greater than about 30 Myr the target star exploded in a supernova before experiencing runaway growth. The collision rates in these clusters were considerably smaller than for clusters with smaller relaxation times (see Fig. 1). As discussed in more detail in §4, the onset of stellar evolution terminates the collision process; premature disruption of the cluster also ends the period of runaway growth.

The 45 N -body calculations listed in Tab. 1 span a broad range of initial conditions. The number of stars varied from 1k (1024) to 64k (65536). Initial density profiles and velocity dispersion for the models were taken from Heggie-Ramamani models (Heggie & Ramamani 1995) with W_0 ranging from 1 to 7. At birth, the clusters were assumed to fill their zero-velocity (Jacobi) surfaces in the Galactic tidal field. In most cases we adopted an initial mass function between $0.1 M_\odot$ and $100 M_\odot$ suggested for the Solar neighborhood by Scalo (1986). However, several calculations were performed using power-law initial mass functions with exponents of -2 or -2.35 (Salpeter) and lower mass limits of $1 M_\odot$. The model with 64k stars (model N64R6r36) was initialized with a Scalo (1986) mass function, but with a lower mass limit of $0.3 M_\odot$ instead of the $0.1 M_\odot$ used in the other models. The characterization of the tidal field is discussed in Portegies Zwart et al. (2001b).

The number of collisions in these simulations ranged from 0 to 24. Fig. 1 shows the mean collision rate $\mathcal{N}_{\text{coll}}$ per star per million years as a function of the initial half-mass relaxation time. The solid line in Fig. 1 is a fit to the simulation data, and has

$$\mathcal{N}_{\text{coll}} = 2.2 \times 10^{-4} \frac{N_{\text{c}}}{t_{\text{rlx}}}, \quad (17)$$

for $t_{\text{rlx}} \lesssim 20 - 30$ Myr, consistent with our earlier estimate (Eq. 8) if $f_{\text{c}} = 0.2$. The quality of the fit in Fig. 1 is quite striking, especially when one bears in mind the rather large spread in initial conditions for the various models.

Figure 2 shows the cumulative mass distributions of the primary (more massive) and secondary (less massive) stars participating in collisions. We include only events in which the secondary experienced its first collision (that is, we omit secondaries which were themselves collision products). In addition, we distinguish between collisions early in the evolution of the cluster and those that happened later by subdividing our data based on the ratio $\tau = t_{\text{coll}}/t_{\text{f}}$, where t_{coll} is the time at which a collision occurred and t_{f} is the dynamical friction time scale of the secondary star (see Eq. 4). The solid lines in Figure 2 show cuts in the secondary masses at $\tau \lesssim 1$, $\tau \lesssim 5$ and $\tau < \infty$ (rightmost line). The mean secondary masses are

Table 1: Overview of the N -body calculations on which the collision rates reported in this paper are based. The first column gives the name of the model, as defined in previous publications (the names RxWx and KMLx are from Portegies Zwart et al. 2001b [see also Portegies Zwart et al. 2001a]; the other models are described in detail by Portegies Zwart et al 1999). The next five columns give the number of stars (in units of 1024), the initial mass function (Scalo 1986, or a power law with slope as indicated), the initial King parameter W_0 , the initial relaxation time (in Myr), and the number of runs performed with these initial conditions (\mathcal{N}_{run}). The final three columns give the average number of collisions in these calculations, the moment the last collision occurred, and the mean collision rate per Myr per star. The models indicated with \star were computed without a Galactic tidal field (see Portegies Zwart et al. 1999).

model	$\langle N \rangle$	IMF	$\langle W_0 \rangle$	$\langle t_{\text{rlx}} \rangle$	\mathcal{N}_{run}	$\langle N_{\text{coll}} \rangle$	$\langle t_{\text{last}} \rangle$	f_{coll}
R34W7	12k	Scalo	7	0.4	2	16.	10.4	-3.90
KML112	4k	-2	7	0.5	2	4.0	1.9	-3.29
KML101	4k	-2	4	1.4	2	2.0	1.0	-3.31
KML142	6k	-2.35	4	1.9	1	1.0	2.2	-4.13
KML111	4k	-2	1	2.3	2	0.5	6.7	-4.74
R90W7	12k	Scalo	7	2.8	1	13.	10.0	-3.98
N64R6r36	64k	Scalo	3	3.2	1	10.	1.0	-3.82
R34W4	12k	Scalo	4	3.2	3	6.3	30.0	-4.71
KML144	14k	-2.35	4	3.9	1	2.0	2.4	-4.24
R150W7	12k	Scalo	7	4.5	2	10.	21.3	-4.42
6k6X5 \star	6k	Scalo	6	5.0	1	21.	47.9	-4.15
R34W1	12k	Scalo	1	5.5	3	4.7	29.1	-4.88
R90W4	12k	Scalo	4	8.1	5	5.8	10.0	-4.33
Nk6X10 \star	9k	Scalo	6	10.0	8	10.	18.0	-4.22
R150W4	12k	Scalo	4	13.0	4	8.5	7.3	-4.02
R90W1	12k	Scalo	1	14.6	1	7.0	9.8	-4.24
6k6X20 \star	6k	Scalo	6	20.0	2	4.0	95.4	-5.17
R150W1	12k	Scalo	1	23.6	2	3.0	2.1	-3.93
R300W4	12k	Scalo	4	55.6	1	1.0	10.0	-5.09
R34W1	32k	Scalo	1	58.1	1	4.0	35.8	-5.47

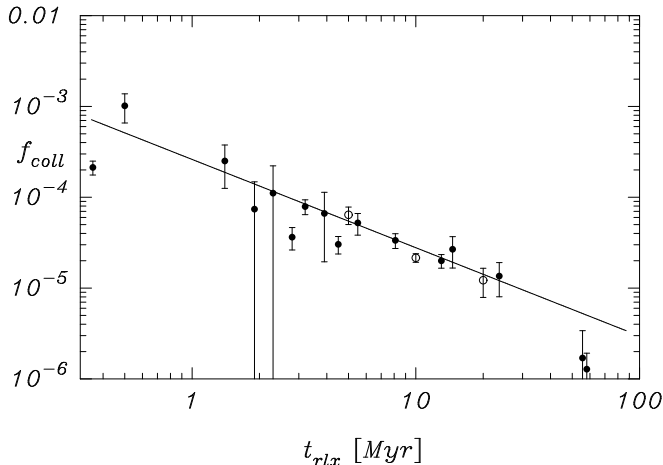


Fig. 1.— Mean collision rate $f_{\text{coll}} = N_{\text{coll}}/N_c t_{\text{last}}$ as function of initial relaxation time for all models of Tab. 1. Here t_{last} is the time of the last collision in the cluster. The open circles give the results of systems which are isolated from the Galactic potential (see Portegies Zwart et al 1999). Vertical bars represent Poissonian 1- σ errors. The solid line is a least squares fit to the data (see Eq. 17). The strong reduction in the collision rate for cluster with an initial relaxation time $t_{\text{rlx}} \gtrsim 30$ Myr is probably real.

$\langle m \rangle = 4.0 \pm 4.8 M_{\odot}$, 8.2 ± 6.5 and $\langle m \rangle = 13.5 \pm 8.8 M_{\odot}$ for $\tau \lesssim 1$, 5 and ∞ , respectively.

The distribution of primary masses in Figure 2 (dashed line) hardly changes as we vary the selection on τ . We therefore show only the full ($\tau \lesssim \infty$) data set for the primaries. In contrast, the distribution of secondary masses changes considerably with increasing τ . For small τ , secondaries are drawn primarily from low-mass stars. As τ increases, the secondary distribution shifts to higher masses while the low-mass part of the distribution remains largely unchanged. The shift from low-mass ($\lesssim 8 M_{\odot}$) to high-mass collision secondaries ($\gtrsim 8 M_{\odot}$) occurs between $\tau = 1$ and $\tau = 5$. This is consistent with the theoretical arguments presented in Sec. 2.3. During the early evolution of the cluster ($\tau \lesssim 1$), collision partners are selected more or less randomly from the available (initial) population in the cluster core; at later times, most secondaries are drawn from the mass-segregated population.

Interestingly, although hard to see in Fig. 2, all the curves are well fit by power laws between $\sim 8 M_{\odot}$ and $\sim 80 M_{\odot}$ ($0.8 M_{\odot}$ and $30 M_{\odot}$ for the leftmost curve). The power-law exponents are -0.4 , -0.5 and -2.3 for $\tau \lesssim 1$, 5, and ∞ , and -0.3 for the primary (dashed) curve. (Note that the Salpeter mass function has exponent -2.35 .)

Figure 3 shows the maximum mass of the runaway collision product as function of the initial mass of the star cluster. Only the left side ($\log M/M_{\odot} \lesssim 7$) of the figure is relevant here; we discuss the extrapolation to larger masses in Sec. 4.3. The N-body results are consistent with the theoretical model presented in Eq. 15.

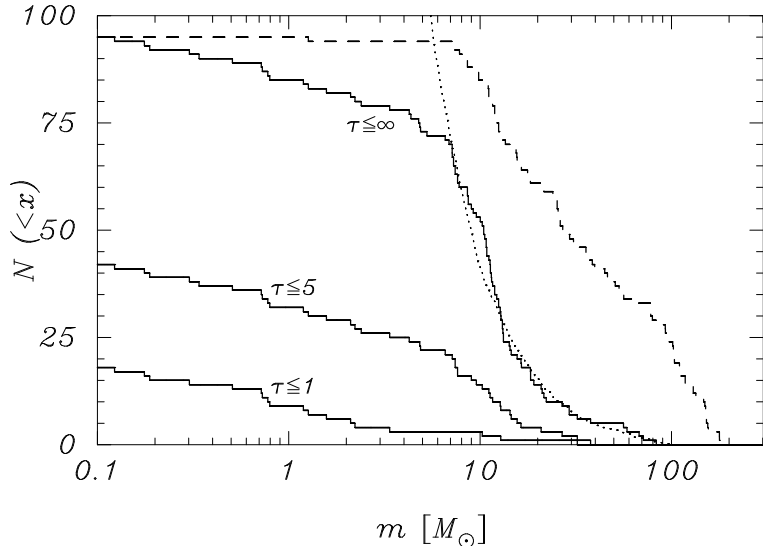


Fig. 2.— Cumulative mass distributions of primary (dashed line) and secondary (solid lines) stars involved in collisions. Only those secondaries experiencing their first collision are included. From left to right, the solid lines represent secondary stars for which $\tau \equiv t_{\text{coll}}/t_f \lesssim 1, 5,$ and ∞ . The numbers of collisions included in each curve are 18 (for $t_{\text{coll}}/t_f \lesssim 1$), 42 and 95 (rightmost two curves). The dotted line gives a Power-law fit with the Salpeter exponent (between $5 M_\odot$ and $100 M_\odot$) to the right most solid curve ($\tau \lesssim \infty$).

4. Discussion

Early core collapse in dense star clusters may initiate a phase of runaway stellar growth, leading to an object containing up to $\sim 0.1\%$ of the total cluster mass. We do not address here the state of this object, which could be a black hole or a star. If the object is a helium- or hydrogen-burning star, it may collapse into a compact object when it exhausts its central fuel. The amount of mass lost in the supernova explosion and whether the compact object receives a velocity kick are important considerations for the future evolution of the collision runaway. An extensive parameter study of the details of the supernova is beyond the scope of this paper. The basis of our analysis, however, is simple and robust to quite substantial perturbations.

We now consider the circumstances under which runaway growth may be prevented or terminated at an early stage. Premature termination of the runaway occurs when stellar mass loss starts to drive the expansion of the star cluster, or when the star cluster is disrupted by external influences. At the end of this section (Sec. 4.3) we briefly discuss the application of runaway growth to the possible formation of supermassive black holes in the bulges of galaxies.

4.1. Prevention of the collision runaway

Runaway growth in a star cluster can only occur when stellar evolution is relatively unimportant compared to the dynamical evolution of the cluster. Stellar mass loss tends to heat the cluster by loss of potential energy, and can easily reverse core collapse. This is particularly true for the most massive stars, which dominate the dynamics of the cluster core and are also the first to lose substantial amounts of mass

in stellar winds and supernovae. The prevention of core collapse also prevents the first or any subsequent collisions, and a reversal of core collapse terminates the collision runaway. As a rule of thumb, we argue that runaway growth can be prevented when the time scale for the most massive stars to segregate to the cluster center exceeds the lifetimes of those stars.

The main-sequence lifetime (t_{ms}) for stars more massive than $\sim 25 M_{\odot}$ is a rather flat function of mass. For high metallicities, the most massive stars ($m \gtrsim 85 M_{\odot}$) actually live longer than stars with masses between 25 and $65 M_{\odot}$ (Meynet et al. 1994). For $Z = 0.04$ (recall that the solar metallicity is $Z_{\odot} = 0.02$), the hydrogen plus helium burning lifetime varies from 6.27 Myr for a $25 M_{\odot}$ star to 7.57 Myr for a $120 M_{\odot}$ star. For low metallicities ($Z = 0.001$), the range becomes 8.19–3.20 Myr for the same masses (see Meynet et al. for details).

For the star cluster to experience core collapse before the most massive stars evolve, we require $t_{\text{cc}} \simeq 0.2 t_{\text{rlx}} \lesssim t_{\text{ms}}(120 M_{\odot}) \sim 3.20\text{--}7.57$ Myr for $Z = 0.001\text{--}0.04$. Runaway growth therefore does not occur in star clusters with initial relaxation times $t_{\text{rlx}} \gtrsim 16\text{--}38$ Myr. For definiteness, we conclude that clusters with $t_{\text{rlx}} \lesssim 25$ Myr experience core collapse before the most massive stars explode, and are therefore prone to runaway collision.

The half-mass radius of a tidally limited cluster expands during core collapse, causing the mean relaxation time to increase by about a factor of 4 (see Portegies Zwart et al. 2001). A cluster with an initial relaxation time of $t_{\text{rlx}} \simeq 25$ Myr will therefore have a relaxation time of about 100 Myr after core collapse. Such a cluster will not experience any further collision runaway, but may still contain the evidence of such a phase in the form of a central compact object with a mass $\lesssim 0.1\%$ of the initial cluster mass. The cluster may also be relatively depleted in low-mass compact objects (stellar mass black holes and neutron stars), as these are consumed during the runaway growth phase (Portegies Zwart et al. 1999).

4.2. Early termination of the runaway by tidal disruption

A star cluster in orbit around the Galactic center is subject to dynamical friction, in much the same way as dynamical friction drives massive stars toward the cluster center. This causes the cluster to spiral into the Galactic center, where it is destroyed (see Gerhard 2001). We derive here in some detail the dynamical friction time scale for a star cluster in the potential of the Galactic center. We assume constant cluster mass M_c , deferring the more realistic case of a time-dependent cluster mass (cf. Eq.13) to McMillan & Portegies Zwart (2002, in preparation).

The drag acceleration due to dynamical friction is (equation [7-18] in Binney & Tremaine, 1987)

$$a = -\frac{4\pi \ln \Lambda_G G^2 M_c \rho_G(R_G)}{v_o^2} \left[\text{erf}(X) - \frac{2X}{\sqrt{\pi}} e^{-X^2} \right]. \quad (18)$$

Here $\ln \Lambda_G$ is the Coulomb logarithm for the Galactic central region, for which we adopt $\ln \Lambda_G \sim R_G/R_c$, erf is the error function and $X \equiv v_o/\sqrt{2}V_G$, where V_G is the one-dimensional velocity dispersion of the stars at distance R_G from the Galactic center.

The mass of the Galaxy lying within the cluster’s orbit at distance R_G ($\lesssim 500$ pc) from the Galactic center is (Sanders & Lowinger 1972; Mezger et al. 1996)

$$M_G(R_G) = 4.25 \times 10^6 \left(\frac{R_G}{1 \text{ pc}} \right)^{1.2} M_{\odot}. \quad (19)$$

Its derivative, the local Galactic density (see Portegies Zwart et al. 2001) is

$$\rho_G(R) \simeq 4.06 \times 10^5 \left(\frac{R_G}{1 \text{ pc}} \right)^{-1.8} \text{ M}_\odot \text{ pc}^{-3}. \quad (20)$$

For inspiral through a sequence of nearly circular orbits, the function $\text{erf}(X) - \frac{2X}{\sqrt{\pi}} \exp(-X^2)$ appearing in Eq. 18 may be determined as follows.

Following Binney & Tremaine (p.226), we write the equation of dynamical equilibrium for stars near the Galactic center as

$$\frac{dP}{dR_G} = -\rho_G \frac{GM_G(R_G)}{R_G^2}, \quad (21)$$

where $P = kT\rho/\langle m \rangle$, $\frac{3}{2}kT = \frac{1}{2}\langle m \rangle \langle v^2 \rangle$. Since $\sigma^2 = \frac{1}{3}\langle v^2 \rangle$, it follows that $P = \sigma^2\rho$, and Eq. 21 becomes

$$\frac{d}{dr}(\sigma^2\rho) = -\frac{\rho}{r}v_o^2, \quad (22)$$

where v_o is the circular orbital velocity at radius R : $V_G^2 = GM_G(R_G)/R_G$. For $M_G \propto R_G^x$ (see Eq.19), and assuming that $V_G^2 \propto v_o^2 \sim R_G^{x-1}$, we find $V_G^2\rho \sim R_G^{2x-4}$, so

$$r \frac{d}{dr}(V_G^2\rho) = (2x - 4)V_G^2\rho = -\rho v_o^2, \quad (23)$$

and hence $X = \sqrt{2-x}$. Eq. 18 then becomes

$$a = -1.2 \ln \Lambda_G \frac{GM_c}{R_G^2} \left[\text{erf}(X) - \frac{2X}{\sqrt{\pi}} \exp(-X^2) \right]. \quad (24)$$

For $x = 1.2$, $X = 0.89$ and

$$a = -0.41 \ln \Lambda_G \frac{GM_c}{R_G^2}. \quad (25)$$

Again following Binney & Tremaine, defining $L = R_G v_o$ and setting $dL/dt = aR_G$, we can integrate Eq.25 with respect to time to find an inspiral time from initial radius R_i of

$$T_f \simeq \frac{1.28}{\ln \Lambda_G} \frac{M_G(R_i)}{M_c} \left[\frac{GM_G(R_i)}{R_i^3} \right]^{-1/2} \quad (26)$$

$$\simeq 1.4 \left(\frac{R_i}{10 \text{ pc}} \right)^{2.1} \left(\frac{10^6 \text{ M}_\odot}{M_c} \right) \text{ Myr} \quad (27)$$

For definiteness, we have assumed $\ln \Lambda_G \sim 4$ ($\Lambda_G \sim R_G/R_c \sim 100$) in Eq. 27, corresponding to a distance of about 10–30 pc from the Galactic center.

The maximum mass of the runaway merger for clusters which are disrupted by inspiral (which of course always destroys the cluster before it reaches the center) may be calculated by replacing t_{disr} in Eq. 15 by T_f . The right-hand side of that equation then becomes a function of

$$\frac{T_f}{t_{\text{cc}}} \simeq 9.0 \left(\frac{R_i}{10 \text{ pc}} \right)^{2.1} \left(\frac{0.25 \text{ pc}}{R_c} \right)^{3/2} \left(\frac{10^5 \text{ M}_\odot}{M_c} \right)^{3/2} \quad (28)$$

We can also estimate the maximum initial distance from the Galactic center for which core collapse occurs (and hence runaway merging may begin) before the cluster disrupts by setting $T_f = t_{\text{cc}}$. The result is $R_i \gtrsim 0.0025 \text{ pc} (R_c M_c / [\text{pc M}_\odot])^{0.71}$. For $R_c = 0.25 \text{ pc}$ and $M_c = 10^5 \text{ M}_\odot$, we find $R_i \gtrsim 3.3 \text{ pc}$.

4.3. Speculation on the formation of supermassive black holes

A million-solar-mass star cluster formed at a distance of $\lesssim 30$ pc from the Galactic center can spiral into the Galactic center by dynamical friction before being disrupted by the tidal field of the Galaxy (see Gerhard 2001). Only the densest star clusters survive to reach the center. These clusters are prone to runaway growth and produce massive compact objects at their centers. Upon arrival at the Galactic center, the star cluster dissolves, depositing its central black hole there. Black holes from in-spiraling star clusters may subsequently merge to form a supermassive black hole. Ebisuzaki et al. (2001) have proposed that such a scenario might explain the presence of the central black hole in the Milky Way galaxy.

If we simply assume that bulges and central supermassive black holes are formed from disrupted star clusters, this model predicts a relation between black hole and bulge masses in galaxies similar to the expression (Eq. 16) connecting the mass of an IMBH to that of its parent cluster. However, the ratio of stellar mass to black-hole mass might be expected to be smaller for galactic bulges than for star clusters, because not all star clusters produce a black hole and not all star clusters survive until the maximum black hole mass is reached. We would expect, however, that the general relation between the black hole mass and that of the bulge remains valid.

Figure 3 shows the relation between the black hole mass and the bulge mass for several Seyfert galaxies and quasars. The expression derived in Sec. 2 and the results of our N -body calculations (Sec. 3) are also indicated. The solid and dashed lines (Eq. 15) fit the N -body calculations and enclose the area of the measured black hole mass–bulge masses. On the way, the solid curve passes through two other black-hole mass estimates, for M82 and the globular cluster M15. We note that the observed relation between bulge and black hole masses has a spread of two orders of magnitude. If this bold extrapolation really does reflect the formation process of bulges and central black holes, this spread could be interpreted as a variation in the efficiency of the runaway merger process. In that case, only about one in a hundred star clusters reaches the galactic center, where its black hole is deposited.

4.4. Is the globular cluster M15 a special case?

The possible black hole in the globular cluster M15 may have been formed by a scenario different from the one described in this paper, as the cluster’s initial relaxation time probably exceeded our upper limit of 25 Myr. The current half-mass relaxation time of M15 is about 2.5 Gyr (Harris 1996), which is far more than our 100 Myr limit for forming a massive central object from a collision runaway.

An alternative is provided by Miller & Hamilton (2001), who describe the formation of massive ($\sim 10^3 M_\odot$) black holes in star clusters with relatively long relaxation times. In their model the black hole grows very slowly over a Hubble time via occasional collisions with other stars, in contrast to the model described here, in which the runaway grows much more rapidly, reaching a characteristic mass of about 0.1% of the total birth mass of the cluster within a few megayears.

One possible way around M15’s long relaxation time may involve the cluster’s rotation. Gebhardt (2000; 2001; private communication) has measured radial velocities of individual stars in the crowded central field, down to two arcsec of the cluster center. He finds that, both in the central part of the cluster ($r < 0.1 r_{\text{hm}}$) and outside the half mass radius, the average rotation velocity is substantial ($v_{\text{rot}} \gtrsim 0.5 \langle v^2 \rangle^{1/2}$). Rotation is quickly lost in a cluster, so to explain a current rotation, M15’s initial rotation rate must probably have been even larger than observed today (see Einsel & Spurzem 1999). Hachisu (1978; 1982)

found, using gaseous cluster models, that an initially rotating cluster tends to evolve into a ‘gravo-gyro catastrophe’ which drives the cluster into core collapse far more rapidly than would occur in a non-rotating system. If the gravo-gyro-driven core collapse occurred within 25 Myr, a collision runaway might have initiated the growth of an intermediate mass black hole in the core of M15.

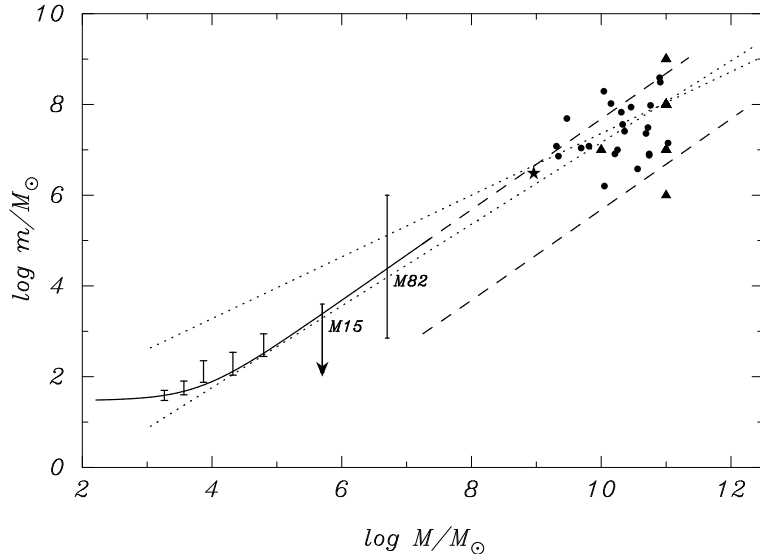


Fig. 3.— The mass after a period of runaway growth as a function of the mass of the star cluster. The solid line is $m_r = 30 + 8 \times 10^{-4} M_{c0} \ln \Lambda_c$ (see Eq. 16 with $f_c = 0.2$, $\gamma = 1$ and $\ln \Lambda_c = \ln M_{c0}/M_\odot$, where M_{c0} is the initial mass of the cluster or $10^6 M_\odot$, whatever is smaller). This relation may remain valid for larger systems built up from many clusters having masses $\lesssim 10^6 M_\odot$. For clusters with $M_{c0} \gtrsim 10^7 M_\odot$ we therefore extend the relation as a dashed line. The logarithmic factor, however, remains constant, as it refers to the clusters out of which the bulge formed, not the bulge itself. The bottom dashed line shows $0.01 m_r$. The five error bars to the left give a summary of the results presented in Table. 1; the data are averages of from left to right: 4k stars (models KML101, KML111 and KML112), 6k (model 6k6X10), 12k (models RxW4 and 12k6X10), 14k (model KML144) and 64k (model N64R6r36). The downward pointed arrow gives the upper limit for the mass of a compact object in the globular cluster M15 (Gebhardt et al. 2000) and the error bar to the right gives the mass estimate for the compact object associated with Chandra source #7 in the irregular Galaxy M82 (Matsumoto & Tsuru 1999). The Milky Way is represented by the asterisk using the bulge mass from Dwek (et al. 1995) and the black hole mass from Eckart & Genzel (1997) and Ghez (2000). Bullets and triangles (upper right) represent the bulge masses and measured black hole mass of Seyfert galaxies and Quasars, respectively (both from Wandel 1999; 2001). The dotted lines gives the range in solutions to a least squares fits to the bullets and triangles (Wandel 2001).

5. Conclusions

We study the runaway growth of a single star in a dense star cluster using a combination of complementary approaches. Our semi-analytic analysis is supported by detailed N -body calculations in which the effects of stellar evolution, stellar dynamics, binary evolution and the perturbing effect of a background Galactic potential are taken self-consistently into account.

Star clusters with initial half-mass relaxation times $t_{\text{rlx}} \lesssim 25$ Myr experience a phase of runaway growth. In this phase a single seed star grows to a mass of about 0.1% of the total mass of the cluster. The first collision occurs at the moment the cluster core collapses. This happens at about $0.2t_{\text{rlx}}$ but no later than about 5 Myr (the evolution time scale for a $\gtrsim 50M_{\odot}$ star). The star which experiences the first collision becomes the target for further collisions, initiating runaway growth. The growth phase is terminated by (1) the disruption of the cluster in the tidal field of the Galaxy (at $t \lesssim 5t_{\text{rlx}}$) or (2) the reversal of core collapse by mass loss from the evolving stellar population (after about 25 Myr).

A star cluster can survive for longer than $5t_{\text{rlx}}$ if, for example, it did not initially fill its Jacobi surface (“Roche lobe”) in the Galactic tidal field. (Examples are NGC 3603 and R 136, the dense star cluster in the 30 Doradus region in the Large Magellanic cloud.) Such clusters go through a phase of runaway stellar growth, but recover after stellar mass loss drives the re-expansion of the cluster core.

From an observational point of view, a tidally limited cluster experiences three very distinct evolutionary phases: a pre-collapse phase until $0.2t_{\text{rlx}}$, a phase of deep core collapse (from $0.2t_{\text{rlx}}$ to about 25 Myr), followed by an expansion phase eventually leading to the disruption of the cluster. During the expansion phase the cluster half-mass radius expands, causing the mean relaxation time to increase by a factor of 4 (see Portegies Zwart et al. 2001). A cluster in this final phase will be observable with a current relaxation time less than $\sim 4 \times 25$ Myr = 100 Myr. The clearest indication of its previous phase of core collapse and runaway growth would be the presence of a central compact object with a mass $\lesssim 0.1\%$ of the initial cluster mass. The cluster may also be relatively depleted in low-mass compact objects (stellar mass black holes and neutron stars), as these are consumed during the runaway growth phase.

Star clusters with an initial relaxation time $t_{\text{rlx}} \gtrsim 25$ Myr do not experience a phase of runaway growth, as core collapse is prevented by mass loss from the most massive stars. These clusters may experience core collapse after ~ 100 Myr, when stellar evolution slows (Takahashi & Portegies Zwart 1999). This later core collapse, however, does not lead to a phase of runaway growth. In such old clusters multiple collisions are still likely to be common and may lead to blue stragglers with a mass more than twice the turn-off mass.

We are grateful to Karl Gebhardt, Ortwin Gerhard, Pranab Ghosh, Douglas Hogg, Piet Hut, Jun Makino, and Rainer Spurzem for discussions and to the anonymous referee for a careful reading of the manuscript. We also thank Tokyo University, the Institute for Advanced Study, the American Museum for Natural History and the University of Indiana for their hospitality and the use of their fabulous GRAPE hardware. This work was supported by NASA ATP grants NAG5-6964 and NAG5-9264, and by the Netherlands Organization for Scientific Research (NWO). SPZ was supported as Hubble Fellow (HF-01112.01-98A) and as fellow of the Royal Netherlands Academy of Arts and Sciences (KNAW).

REFERENCES

- Antonov, V. A. 1962, Solution of the problem of stability of stellar system Emden’s density law and the spherical distribution of velocities, *Vestnik Leningradskogo Universiteta*, Leningrad: University, 1962
- Binney, J., Tremaine, S. 1987, *Galactic dynamics*, Princeton, NJ, Princeton University Press, 1987, 747 p.
- Chernoff, D. F., Weinberg, M. D. 1990, *ApJ*, 351, 121
- Cohn, H. 1980, *ApJ*, 242, 765

- Dwek, E., Arendt, R. G., Hauser, M. G., Kelsall, T., Lisse, C. M., Moseley, S. H., Silverberg, R. F., Sodroski, T. J., Weiland, J. L. 1995, *ApJ*, 445, 716
- Eckart, A., Genzel, R. 1997, *MNRAS*, 284, 576
- Einsel, C., Spurzem, R. 1999, *MNRAS*, 302, 81
- Fabbiano, G., Zezas, A., Murray, S. S. 2001, *ApJ*, 554, 1035
- Freitag, M., Benz, W. 2001, *A&A*, 375, 711
- Gebhardt, K., Pryor, C., O'Connell, R. D., Williams, T. B., Hesser, J. E. 2000, *AJ*, 119, 1268
- Gerhard, O. 2001, *ApJ*, 546, L39
- Gerssen, J., van der Marel, R. P., Dubath, P., Gebhardt, K., Guhathakurta, P., Peterson, R., Pryor, C. 2001, American Astronomical Society Meeting
- Ghez, A. M., Klein, B. L., Morris, M., Becklin, E. E. 1998, *ApJ*, 509, 678
- Goodman, J. 1987, *ApJ*, 313, 576
- Hachisu, I. 1979, *PASJ*, 31, 523
- Hachisu, I. 1982, *PASJ*, 34, 313
- Harris, W. E. 1996, *VizieR Online Data Catalog*
- Heggie, D. C., Ramamani, N. 1995, *MNRAS*, 272, 317
- Hut, P., Inagaki, S. 1985, *ApJ*, 298, 502
- Joshi, K. J., Nave, C. P., Rasio, F. A. 2001, *ApJ*, 550, 691
- Kaaret, P., Prestwich, A. H., Zezas, A., Murray, S. S., Kim, D.-W., Kilgard, R. E., Schlegel, E. M., Ward, M. J. 2000, *AAS/High Energy Astrophysics Division*, 32, 1511
- Kaaret, P., Prestwich, A. H., Zezas, A., Murray, S. S., Kim, D.-W., Kilgard, R. E., Schlegel, E. M., Ward, M. J. 2001, *MNRAS*, 321, L29
- King, A. R., Davies, M. B., Ward, M. J., Fabbiano, G., Elvis, M. 2001, *ApJ*, 552, L109
- King, I. R. 1966, *AJ*, 71, 64
- Kotoku, J., Mizuno, T., Kubota, A., Makishima, K. 2000, *PASJ*, 52, 1081
- Lee, H. M. 1987, *ApJ*, 319, 801
- Makino, J. 1996, *ApJ*, 471, 796
- Makino, J. 2001, in *ASP Conf. Ser. 228: Dynamics of Star Clusters and the Milky Way*, 87
- Makino, J., Hut, P. 1990, *ApJ*, 365, 208
- Makino, J., Taiji, M., Ebisuzaki, T., Sugimoto, D. 1997, *ApJ*, 480, 432

- Matsumoto, H., Canizares, C. R., Tsuru, T. G., Koyama, K., Awaki, H., Matsushita, S., Prestwitch, A., Zezas, A. L., Kawai, N., Ward, M., Kawabe, R. 2000, AAS/High Energy Astrophysics Division, 32, 0108
- Matsumoto, H., Tsuru, T. G., Koyama, K., Awaki, H., Canizares, C. R., Kawai, N., Matsushita, S., Kawabe, R. 2001, ApJ, 547, L25
- Matsushita, S., Kawabe, R., Matsumoto, H., Tsuru, T. G., Kohno, K., Morita, K., Okumura, S. K., Vila-Vilaró, B. 2000, ApJ, 545, L107
- McMillan, S. L. W. 1986, ApJ, 306, 552
- Mengel, S., Lehnert, M. D., Thatte, N., Tacconi-Garman, L. E., Genzel, R. 2001, ApJ, 550, 280
- Meynet, G., Maeder, A., Schaller, G., Schaerer, D., Charbonnel, C. 1994, A&AS, 103, 97
- Mezger, P. G., Duschl, W. J., Zylka, R. 1996, A&A Rev., 7, 289
- Miller, C. M., Hamilton, D. P. 2001, in astro-ph/0106188
- Mizuno, T., Ohnishi, T., Kubota, A., Makishima, K., Tashiro, M. 1999a, Astronomische Nachrichten, 320, 356
- Mizuno, T., Ohnishi, T., Kubota, A., Makishima, K., Tashiro, M. 1999b, PASJ, 51, 663
- Portegies Zwart, S. F., Makino, J., McMillan, S. L. W., Hut, P. 1999, A&A, 348, 117
- Portegies Zwart, S. F., Makino, J., McMillan, S. L. W., Hut, P. 2001a, ApJ, 546, L101
- Portegies Zwart, S. F., McMillan, S. L. W. 2000, ApJ, 528, L17
- Portegies Zwart, S. F., McMillan, S. L. W., Hut, P., Makino, J. 2001b, MNRAS, 321, 199
- Quinlan, G. D., Shapiro, S. L. 1990, ApJ, 356, 483
- Salpeter, E. E. 1955, ApJ, 121, 161
- Sanders, R. H. 1970, ApJ, 162, 791
- Sanders, R. H., Lowinger, T. 1972, AJ, 77, 292
- Scalo, J. M. 1986, Fund. of Cosm. Phys., 11, 1
- Spitzer, L. 1987, Dynamical evolution of globular clusters, Princeton, NJ, Princeton University Press, 1987, p. 191
- Spitzer, L. J. 1969, ApJ, 158, L139
- Spitzer, L. J., Hart, M. H. 1971, ApJ, 164, 399
- Takahashi, K., Portegies Zwart, S. F. 1998, ApJ, 503, L49
- Vishniac, E. T. 1978, ApJ, 223, 986
- Wandel, A. 1999, ApJ, 519, L39

Wandel, A. 2001, in astro-ph/0108461, 8461

Zezas, A., Fabbiano, G. 2002, in astro-ph/0202176

Zezas, A., Fabbiano, G., Rots, A. H., Murray, S. S. 2002, in astro-ph/0203174